

Yoshizawa’s cross-helicity effect and its quenching

A. BRANDENBURG†§ and K.-H. RÄDLER‡ *

†NORDITA, Roslagstullsbacken 23, SE-10691 Stockholm, Sweden

§Department of Astronomy, Stockholm University, SE-10691 Stockholm, Sweden

‡Astrophysical Institute Potsdam, An der Sternwarte 16, D-14482 Potsdam, Germany

(July 31, 2021)

A central quantity in mean-field magnetohydrodynamics is the mean electromotive force $\overline{\mathcal{E}}$, which in general depends on the mean magnetic field. It may however also have a part independent of the mean magnetic field. Here we study an example of a rotating conducting body of turbulent fluid with non-zero cross-helicity, in which a contribution to $\overline{\mathcal{E}}$ proportional to the angular velocity occurs (Yoshizawa 1990). If the forcing is helical, it also leads to an α effect, and large-scale magnetic fields can be generated. For not too rapid rotation, the field configuration is such that Yoshizawa’s contribution to $\overline{\mathcal{E}}$ is considerably reduced compared to the case without α effect. In that case, large-scale flows are also found to be generated.

Keywords: Mean-field dynamo; rotating turbulence; cross-helicity effect; alpha effect

1 Introduction

Many studies of the large-scale magnetic fields in turbulent astrophysical bodies such as the Sun or the Galaxy are carried out in the framework of mean-field electrodynamics (see the textbooks by Moffatt 1978, Parker 1978, Krause and Rädler 1980, Zeldovich *et al.* 1983). It is based on the induction equation governing the magnetic field \mathbf{B} ,

$$\frac{\partial \mathbf{B}}{\partial t} = \nabla \times (\mathbf{U} \times \mathbf{B} - \eta \mu_0 \mathbf{J}), \quad (1)$$

where \mathbf{U} is the fluid velocity, $\mathbf{J} = \nabla \times \mathbf{B} / \mu_0$ the current density, where \mathbf{U} is the fluid velocity, $\mathbf{J} = \nabla \times \mathbf{B} / \mu_0$ is the current density, η the magnetic diffusivity, and μ_0 the vacuum permeability. Both the magnetic field \mathbf{B} and the velocity field \mathbf{U} are considered sums of mean parts, $\overline{\mathbf{B}}$ and $\overline{\mathbf{U}}$, defined as proper averages of the original fields, and fluctuations. The averages are assumed to satisfy the Reynolds averaging rules. The mean magnetic field $\overline{\mathbf{B}}$ then obeys the mean-field induction equation

$$\frac{\partial \overline{\mathbf{B}}}{\partial t} = \nabla \times (\overline{\mathbf{U}} \times \overline{\mathbf{B}} + \overline{\mathcal{E}} - \eta \mu_0 \overline{\mathbf{J}}). \quad (2)$$

Here $\overline{\mathcal{E}} = \overline{\mathbf{u} \times \mathbf{b}}$ is the mean electromotive force resulting from the fluctuations of velocity and magnetic field, $\mathbf{u} = \mathbf{U} - \overline{\mathbf{U}}$ and $\mathbf{b} = \mathbf{B} - \overline{\mathbf{B}}$. Generally, $\overline{\mathcal{E}}$ can be represented as a sum

$$\overline{\mathcal{E}} = \overline{\mathcal{E}}^{(0)} + \overline{\mathcal{E}}^{(B)} \quad (3)$$

*Corresponding author. Email: brandenb@nordita.org

of a part $\overline{\mathcal{E}}^{(0)}$, which is independent of $\overline{\mathbf{B}}$, and a part $\overline{\mathcal{E}}^{(B)}$ vanishing with $\overline{\mathbf{B}}$. In many representations and applications of mean-field electrodynamics the part $\overline{\mathcal{E}}^{(0)}$ of $\overline{\mathcal{E}}$ is ignored. Only the part $\overline{\mathcal{E}}^{(B)}$, which is of crucial importance for dynamo action, is taken into account.

Here we focus our attention on the part $\overline{\mathcal{E}}^{(0)}$ of $\overline{\mathcal{E}}$. It may depend on non-magnetic quantities influencing the turbulence, in general also on $\overline{\mathbf{U}}$. If the magnitude of $\overline{\mathbf{U}}$ is small, and if $\overline{\mathbf{U}}$ varies only weakly in space and time, we may write

$$\overline{\mathcal{E}}_i^{(0)} = \overline{\mathcal{E}}_i^{(00)} + \Xi_{ij}\overline{U}_j + \Upsilon_{ijk}\overline{U}_{j,k} \quad (4)$$

with $\overline{\mathcal{E}}_i^{(00)}$ as well as Ξ_{ij} and Υ_{ijk} being independent of $\overline{\mathbf{U}}$. Of course, the contribution $\overline{\mathcal{E}}^{(00)}$ to $\overline{\mathcal{E}}^{(0)}$ can only be non-zero if the turbulence allows us to define a direction. For example, turbulence in a rotating body shows in general an anisotropy determined by the angular velocity $\boldsymbol{\Omega}$, and $\overline{\mathcal{E}}^{(00)}$ might then be proportional to $\boldsymbol{\Omega}$, say equal to $c_\Omega\boldsymbol{\Omega}$. The Ξ_{ij} term in (4) can only be unequal to zero if the turbulence lacks Galilean invariance. In the case of isotropic turbulence it describes a contribution to $\overline{\mathcal{E}}^{(0)}$ proportional to $\overline{\mathbf{U}}$, say equal to $c_U\overline{\mathbf{U}}$. Note that in forced turbulence Galilean invariance can be broken if, independent of the flow, the forcing is fixed in space and shows a finite correlation time (for an example see Rädler and Brandenburg 2010). The Υ_{ijk} term, if restricted to isotropic turbulence, corresponds to a contribution to $\overline{\mathcal{E}}^{(0)}$ proportional to $\nabla \times \overline{\mathbf{U}}$, say equal to $c_W\nabla \times \overline{\mathbf{U}}$. The coefficients c_Ω and c_W are, in contrast to c_U , pseudoscalars. The contributions $c_\Omega\boldsymbol{\Omega}$ and $c_W\nabla \times \overline{\mathbf{U}}$ to the mean electromotive force were first considered by Yoshizawa (1990). He found that both c_Ω and c_W are closely connected with the cross helicity $\overline{\mathbf{u} \cdot \mathbf{b}}$. In what follows the occurrence of the contributions $c_\Omega\boldsymbol{\Omega}$ and $c_W\nabla \times \overline{\mathbf{U}}$ to the mean electromotive force $\overline{\mathcal{E}}$ is called ‘‘Yoshizawa effect’’. This effect has been invoked to explain magnetic fields in accretion discs (Yoshizawa and Yokoi 1993) and spiral galaxies (Yokoi 1996). It has also been used to explain the surprisingly high level of magnetic fields in young galaxies (Brandenburg and Urpin 1998), because the amplification of the mean field by this effect is independent of any seed magnetic field. The equivalence of a rotation of the frame of reference with a rotation of the fluid body might suggest an equality of c_Ω and $2c_W$. However, this equivalence exists only in pure hydrodynamics, which is governed by the momentum equation, but no longer in magnetohydrodynamics, where both the momentum equation and the induction equation are important. As a consequence, c_Ω is in general different from $2c_W$, see Rädler and Brandenburg (2010), in particular the discussion at the end of Section 3.1.

As for the part $\overline{\mathcal{E}}^{(B)}$ of $\overline{\mathcal{E}}$, we recall here the traditional ansatz

$$\overline{\mathcal{E}}^{(B)} = \alpha_{ij}\overline{B}_j + \eta_{ijk}\overline{B}_{j,k}. \quad (5)$$

It can be justified for cases in which $\overline{\mathbf{B}}$ varies only slowly in space and time. In the simple case of isotropic turbulence it takes the form $\overline{\mathcal{E}}^{(B)} = \alpha\overline{\mathbf{B}} - \eta_t\nabla \times \overline{\mathbf{B}}$, which describes the α effect and the occurrence of a turbulent magnetic diffusivity (Krause and Rädler 1980).

In this article, we report on numerical simulations of magnetohydrodynamic turbulence in a rotating body, that is, under the influence of the Coriolis force. We present results for the mean electromotive force and discuss them in the light of the above remarks, focussing particular attention on the Yoshizawa effect.

2 Model

We consider forced magnetohydrodynamic turbulence of an electrically conducting, compressible, rotating fluid which is permeated by a magnetic field. An isothermal equation of state is used so that the pressure p and the mass density ρ are proportional to each other, $p = \rho c_s^2$, with c_s being a constant sound speed. The magnetic field \mathbf{B} , the fluid velocity \mathbf{U} and the mass density ρ are assumed to obey

$$\frac{\partial \mathbf{A}}{\partial t} = \mathbf{U} \times \mathbf{B} - \eta\mu_0\mathbf{J} + \mathbf{f}_M, \quad (6)$$

$$\frac{D\mathbf{U}}{Dt} = -c_s^2 \nabla \ln \rho - 2\boldsymbol{\Omega} \times \mathbf{U} + \frac{1}{\rho} \mathbf{J} \times \mathbf{B} + \frac{1}{\rho} \nabla \cdot 2\rho\nu\mathbf{S} + \mathbf{f}_K, \quad (7)$$

$$\frac{D \ln \rho}{Dt} = -\nabla \cdot \mathbf{U}. \quad (8)$$

Unless indicated otherwise, we exclude a homogeneous part of the magnetic field. \mathbf{A} is the magnetic vector potential, $\nabla \times \mathbf{A} = \mathbf{B}$, and η again the magnetic diffusivity, $D/Dt = \partial/\partial t + \mathbf{U} \cdot \nabla$ is the advective time derivative, $\boldsymbol{\Omega}$ the angular velocity which defines the Coriolis force, $S_{ij} = \frac{1}{2}(U_{i,j} + U_{j,i}) - \frac{1}{3}\delta_{ij} \nabla \cdot \mathbf{U}$ the trace-less rate of strain tensor, ν the kinematic viscosity, while \mathbf{f}_M and \mathbf{f}_K define the magnetic and kinetic forcings specified below. The simultaneous magnetic and kinetic forcing is a simple way to generate non-zero cross helicity. We admit only small Mach numbers, that is, only weak compressibility effects.

Equation (6)–(8) are solved numerically in a cubic domain with the edge length L assuming periodic boundary conditions. Then $k_1 = 2\pi/L$ is the smallest possible wavenumber. We assume that $\boldsymbol{\Omega}$ is parallel to the positive z direction, that is, $\boldsymbol{\Omega} = (0, 0, \Omega)$ with $\Omega > 0$.

With the intention to approximate a forcing that is δ -correlated in time we add after each time step of duration δt the contributions $\delta t \mathbf{f}_M$ and $\delta t \mathbf{f}_K$ to \mathbf{A} and \mathbf{U} , respectively, and change \mathbf{f}_M and \mathbf{f}_K randomly from one step to the next (Brandenburg 2001). We define them until further notice by putting

$$\mathbf{f}_M = N_M \text{Re}\{\tilde{\mathbf{f}}_{\mathbf{k}(t)} \exp[i\mathbf{k}(t) \cdot \mathbf{x} + i\phi(t)]\}, \quad \mathbf{f}_K = N_K \text{Re}\{i\mathbf{k}(t) \times \tilde{\mathbf{f}}_{\mathbf{k}(t)} \exp[i\mathbf{k}(t) \cdot \mathbf{x} + i\phi(t)]\}. \quad (9)$$

Here N_M and N_K are given by

$$N_M = \mathcal{N}_M c_s \sqrt{\mu_0 \rho_0 c_s / k_f \delta t}, \quad N_K = \mathcal{N}_K c_s \sqrt{c_s / k_f \delta t}, \quad (10)$$

where \mathcal{N}_M and \mathcal{N}_K are dimensionless amplitudes, ρ_0 is the initial mass density, considered as uniform, k_f the average forcing wavenumber and δt the duration of the time step. Further $\tilde{\mathbf{f}}_{\mathbf{k}}$ is given by

$$\tilde{\mathbf{f}}_{\mathbf{k}} = \frac{\mathbf{f}_{\mathbf{k}(t)} - i\varepsilon \hat{\mathbf{k}}(t) \times \mathbf{f}_{\mathbf{k}(t)}}{\sqrt{1 + \varepsilon^2}}, \quad (11)$$

where $\mathbf{f}_{\mathbf{k}}$, considered as a function of \mathbf{k} , is a statistically homogeneous isotropic non-helical random vector field, $\hat{\mathbf{k}}$ is the unit vector $\mathbf{k}/|\mathbf{k}|$ and ε a parameter satisfying $|\varepsilon| \leq 1$ (Haugen *et al.* 2004). Then $\tilde{\mathbf{f}}_{\mathbf{k}}$ is non-helical if $\varepsilon = 0$, and maximally helical if $|\varepsilon| = 1$. We consider the wavevector \mathbf{k} and the phase ϕ as random functions of time, $\mathbf{k} = \mathbf{k}(t)$ and $\phi = \phi(t)$, such that their values within a given time step are constant, but change at the end of it and take then other values that are not correlated with them. We further put

$$\mathbf{f}_{\mathbf{k}(t)} = \frac{\mathbf{k}(t) \times \mathbf{e}(t)}{\sqrt{\mathbf{k}(t)^2 - (\mathbf{k}(t) \cdot \mathbf{e}(t))^2}}, \quad (12)$$

where $\mathbf{e}(t)$ is a unit vector which is in the same sense random as $\mathbf{k}(t)$ but not parallel to it. In this way we have $\nabla \cdot \mathbf{f}_M = \nabla \cdot \mathbf{f}_K = 0$. The wavevectors \mathbf{k} are chosen such that their moduli $k = |\mathbf{k}|$ lie in a band of width δk around a mean forcing wavenumber k_f , that is, $k_f - \delta k/2 \leq k \leq k_f + \delta k/2$, and we choose $\delta k = k_1$. In the limit of small time steps, which we approach in our calculations, the forcing may be considered as δ -correlated. The fluid flow is then Galilean invariant, because due to the lack of memory of the forcing one cannot distinguish between a forcing that is advected with the flow from one that is not.

We describe our simulations using the magnetic Prandtl number Pr_M , the Coriolis number Co , the magnetic Reynolds number Re_M , and the Lundquist number Lu ,

$$\text{Pr}_M = \nu/\eta, \quad \text{Co} = 2\Omega/u_{\text{rms}}k_f, \quad \text{Re}_M = u_{\text{rms}}/\eta k_f, \quad \text{Lu} = b_{\text{rms}}/\sqrt{\mu_0 \rho_0} \eta k_f, \quad (13)$$

with u_{rms} and b_{rms} being defined using averages over the full computational volume. While Pr_M and Co are input parameters, Re_M and Lu are used for describing results. For our numerical simulations we use the PENCIL CODE¹, which is a high-order public domain code (sixth order in space and third order in time) for solving partial differential equations, including the hydromagnetic equations given above.

3 Results and Interpretation

We have performed a series of simulations with $\text{Pr}_M = 1$, $\mathcal{N}_K = 0.01$, $\mathcal{N}_M = 0.005$, $k_f = 5k_1$ and varying Co . As initial conditions we used $\mathbf{U} = \mathbf{A} = \mathbf{0}$ and $\rho = \rho_0$.

We discuss the results here in terms of space averages taken over the full computational volume defined above and denoted by angle brackets. More precisely, we now put, e.g., $\bar{\mathbf{U}}$ and $\bar{\mathbf{B}}$ equal to $\langle \mathbf{U} \rangle$ and $\langle \mathbf{B} \rangle$. Of course, quantities like $\langle \mathbf{U} \rangle$ and $\langle \mathbf{B} \rangle$ are independent of space coordinates. We have further $\mathbf{B} = \langle \mathbf{B} \rangle + \mathbf{b}$ and $\mathbf{U} = \langle \mathbf{U} \rangle + \mathbf{u}$. Using $\mathbf{B} = \nabla \times \mathbf{A}$ and the periodicity of \mathbf{A} , we have $\langle \mathbf{B} \rangle = \mathbf{0}$, that is, $\mathbf{B} = \mathbf{b}$. By contrast, $\langle \mathbf{U} \rangle$ is not necessarily equal to zero. $\langle \mathbf{B} \rangle = \mathbf{0}$ is however enough to justify $\langle \mathbf{U} \cdot \mathbf{B} \rangle = \langle \mathbf{u} \cdot \mathbf{b} \rangle$ and $\langle \mathbf{U} \times \mathbf{B} \rangle = \langle \mathbf{u} \times \mathbf{b} \rangle$.

Within this framework the mean electromotive force discussed above and denoted there by $\bar{\mathcal{E}}$ is equal to $\langle \mathbf{u} \times \mathbf{b} \rangle$. According to the ideas expressed in the Introduction, and recalling that volume averages of spatial derivatives of our periodic variables \mathbf{A} or \mathbf{U} vanish, we expect

$$\langle \mathbf{u} \times \mathbf{b} \rangle = c_\Omega \boldsymbol{\Omega} + c_U \langle \mathbf{U} \rangle \quad (14)$$

with c_Ω determined by the cross-helicity $\langle \mathbf{u} \cdot \mathbf{b} \rangle$. Owing to Galilean invariance of the flow in our model c_U should vanish. In all simulations under the mentioned conditions $\langle \mathbf{U} \rangle$ turned out very small. Even if the initial condition for \mathbf{U} was changed and larger $|\langle \mathbf{U} \rangle|$ were thereby generated, no influence of $\langle \mathbf{U} \rangle$ on $\langle \mathbf{u} \times \mathbf{b} \rangle$ was observed. We conclude from this that indeed $c_U = 0$.

Let us give further results first for non-helical forcing, $\varepsilon = 0$. In this case we expect no α effect and see no reason for the generation of large-scale magnetic fields. Figure 1 gives Re_M and Lu , here considered as measures for u_{rms} and b_{rms} , as functions of Co . Figure 2 shows that the cross helicity $\langle \mathbf{u} \cdot \mathbf{b} \rangle$ and, if $\text{Co} \neq 0$, also the z component of the mean electromotive force $\langle \mathbf{u} \times \mathbf{b} \rangle$ are non-zero. The moduli of the x and y components of $\langle \mathbf{u} \times \mathbf{b} \rangle$ are negligible. According to Yoshizawa's result we expect $\langle \mathbf{u} \times \mathbf{b} \rangle_z = \frac{1}{2} \zeta \langle \mathbf{u} \cdot \mathbf{b} \rangle \text{Co}$ with ζ being a number of the order of unity. Figure 3 shows that $\langle \mathbf{u} \times \mathbf{b} \rangle_z / \langle \mathbf{u} \cdot \mathbf{b} \rangle \text{Co}$ is indeed around 0.5 as long as Co is small. The decay with growing Co might be a result of strong rotational quenching of $\langle \mathbf{u} \times \mathbf{b} \rangle_z$.

Consider next the case of maximally helical forcing, $\varepsilon = 1$. The simulations for this case have been carried out with a modified definition of \mathbf{f}_K . In (9) and (10), $i\mathbf{k}(t) \times \tilde{\mathbf{f}}_{\mathbf{k}(t)}$ has been replaced by $\tilde{\mathbf{f}}_{\mathbf{k}(t)}$, and $\sqrt{c_s/k_f \delta t}$ by $\sqrt{c_s k_f / \delta t}$. Now an α effect is to be expected and, as a consequence, the generation of magnetic fields with scales comparable to that of the computational domain (Brandenburg 2001). Indeed, as illustrated by Figure 4, different types of large-scale magnetic fields with a dominant wavenumber $k = k_1$ occur. Following Hubbard *et al.* (2009), we call them “meso-scale fields”. As can be seen in the example of Figure 5, these fields are to a good approximation of Beltrami shape. Three different types of such fields have been observed,

$$\mathbf{B}^X = B_0(0, \sin k_1 x, \cos k_1 x), \quad \mathbf{B}^Y = B_0(\cos k_1 y, 0, \sin k_1 y), \quad \mathbf{B}^Z = B_0(\sin k_1 z, \cos k_1 z, 0), \quad (15)$$

in general with common phase shifts of the components in the x , y and z directions. B_0 was always of the order of several equipartition values B_{eq} , defined by $B_{\text{eq}} = \sqrt{\mu_0 \rho_0} u_{\text{rms}}$. For not too large Co all three types, \mathbf{B}^X , \mathbf{B}^Y and \mathbf{B}^Z , turned out to be possible, but for Co exceeding a value of about unity only that of type \mathbf{B}^Z occurs. This becomes understandable when considering that for the amplification of meso-scale

¹<http://pencil-code.googlecode.com/>

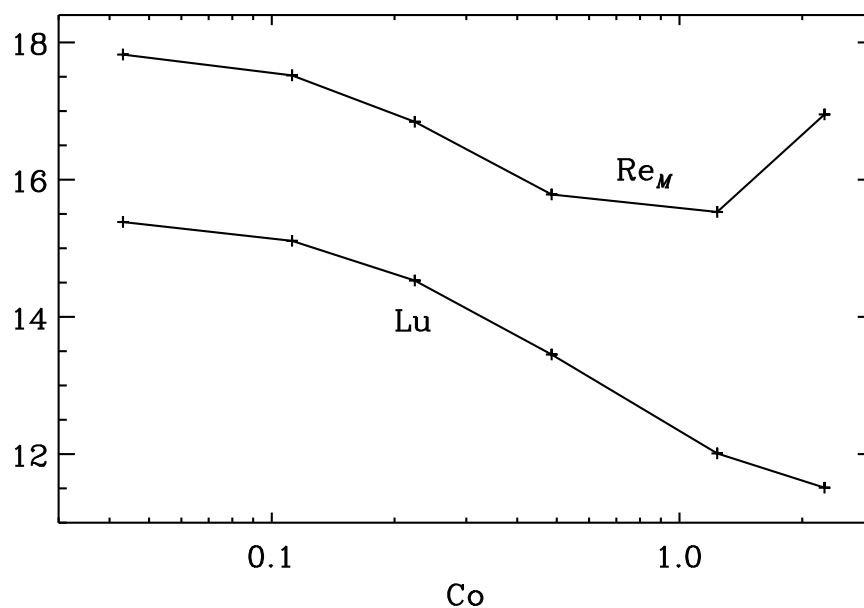


Figure 1. Non-helical case. Dependence of Re_M and Lu on Co for fixed forcing amplitudes, as specified in the text.

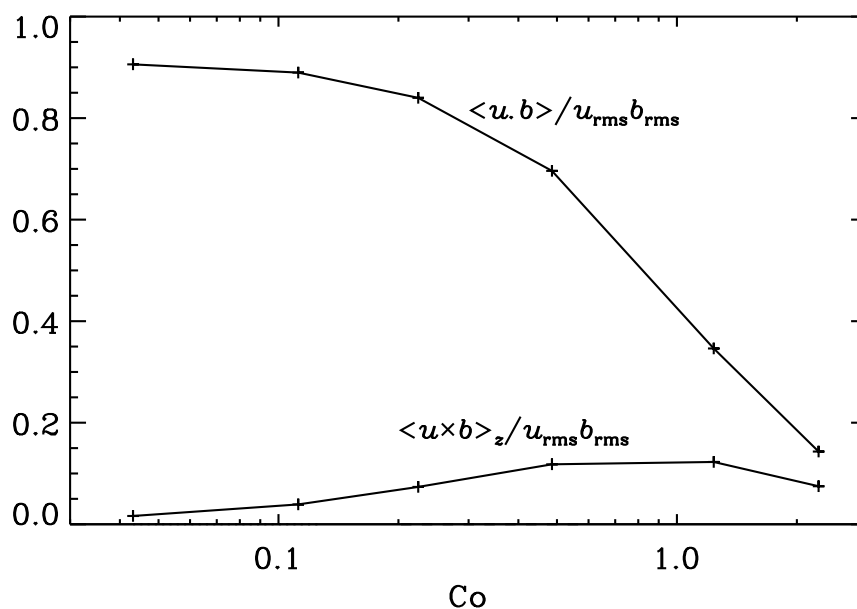


Figure 2. Non-helical case. Normalized cross helicity $\langle \mathbf{u} \cdot \mathbf{b} \rangle / u_{rms} b_{rms}$ and z component of normalized mean electromotive force $\langle \mathbf{u} \times \mathbf{b} \rangle_z / u_{rms} b_{rms}$ as functions of Co . The moduli of the x and y components of $\langle \mathbf{u} \times \mathbf{b} \rangle / u_{rms} b_{rms}$ are below 10^{-3} .

fields of type \mathbf{B}^X and \mathbf{B}^Y , the products $\alpha_{yy}\alpha_{zz}$ and $\alpha_{xx}\alpha_{zz}$ are important, while for \mathbf{B}^Z it is $\alpha_{xx}\alpha_{yy}$, but $|\alpha_{zz}|$ is reduced by rotational quenching (Rüdiger 1978) for large values of Co .

Furthermore, meso-scale flows of type \mathbf{U}^X and \mathbf{U}^Y , defined analogously to (15), are also possible; see the lower panels of Figure 4. Such flows have never been seen in the absence of cross helicity. They could be, e.g., a consequence of the Lorentz force due to the meso-scale magnetic fields, or of a contribution to the Reynolds stresses which exists only for non-zero cross helicity, in particular terms linearly proportional to derivatives of the mean magnetic field (Rheinhardt and Brandenburg 2010, Yokoi 2011). Revealing the nature of these flows requires further investigation. Remarkably, already for small Co it seems impossible to tolerate \mathbf{U}^Z flows. This might be connected with the fact that the Coriolis force acting on a \mathbf{U}^Z flow would produce a 90° phase-shifted flow proportional to $(\cos k_1 z, -\sin k_1 z, 0)$. By comparison, the Coriolis

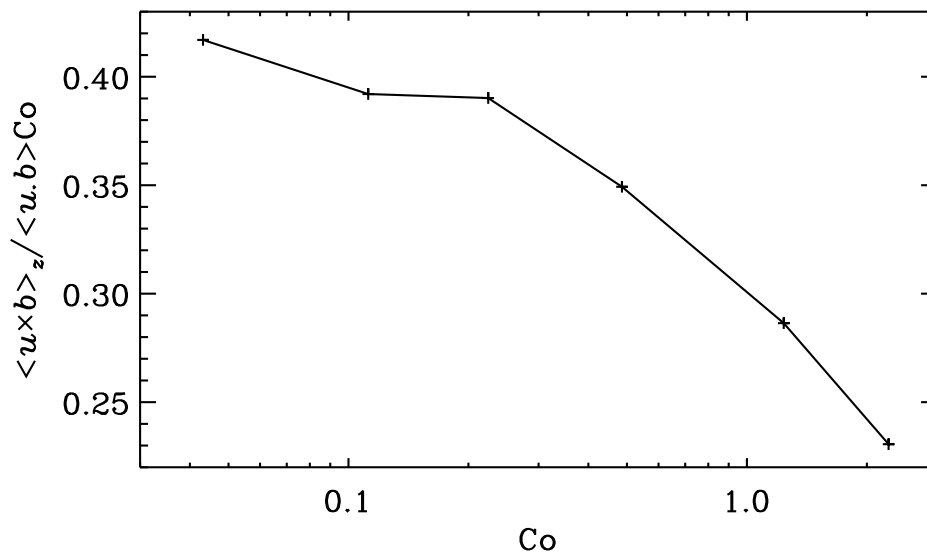


Figure 3. Non-helical case. Dependence of $\langle \mathbf{u} \times \mathbf{b} \rangle_z / \langle \mathbf{u} \cdot \mathbf{b} \rangle Co$ on Co .

force acting on a \mathbf{U}^X or a \mathbf{U}^Y flow gives another one proportional to $(\sin k_1 x, 0, 0)$ or $(0, -\cos k_1 y, 0)$, respectively, which does not directly interfere with \mathbf{U}^X or \mathbf{U}^Y .

Both the cross helicity $\langle \mathbf{u} \cdot \mathbf{b} \rangle$ and the mean electromotive force $\langle \mathbf{u} \times \mathbf{b} \rangle$ are influenced by the presence of the meso-scale magnetic fields and meso-scale flows. Figure 6 shows the dependence of $\langle \mathbf{u} \cdot \mathbf{b} \rangle$ and $\langle \mathbf{u} \times \mathbf{b} \rangle_z$ on the types of the meso-scale magnetic fields and on Co . Meso-scale magnetic fields of \mathbf{B}^X or \mathbf{B}^Y type together with meso-scale flows enhance the level of $\langle \mathbf{u} \cdot \mathbf{b} \rangle / u_{\text{rms}} b_{\text{rms}}$, especially for small values of Co . With meso-scale magnetic fields of \mathbf{B}^Z type $\langle \mathbf{u} \cdot \mathbf{b} \rangle / u_{\text{rms}} b_{\text{rms}}$ is reduced relative to that in the non-helical case (Figure 2), because b_{rms} is enhanced by a factor of about 2. As Figure 7 demonstrates, $\langle \mathbf{u} \times \mathbf{b} \rangle_z / \langle \mathbf{u} \cdot \mathbf{b} \rangle Co$ depends now crucially on whether meso-scale fields of \mathbf{B}^X or \mathbf{B}^Y type or of \mathbf{B}^Z type are present. In the first case the Yoshizawa effect is clearly reduced by the meso-scale fields; in the second case it is enhanced for small Co , but reduced for larger Co .

The remarkable strength of the meso-scale fields can lead to strong magnetic quenching effects. As a first approach to the understanding of such effects the non-helical case has been studied with an imposed homogeneous magnetic field in the y or z directions, $(0, B_0, 0)$ or $(0, 0, B_0)$, respectively. Figure 8 shows as an example the dependence of $\langle \mathbf{u} \times \mathbf{b} \rangle_z / \langle \mathbf{u} \cdot \mathbf{b} \rangle Co$ at $Co \approx 0.25$ on B_0 / B_{eq} . It suggests that in the helical case the reduction of $\langle \mathbf{u} \times \mathbf{b} \rangle_z / \langle \mathbf{u} \cdot \mathbf{b} \rangle Co$ by \mathbf{B}^X or \mathbf{B}^Y fields, which possess a non-zero z component, is stronger than that by \mathbf{B}^Z fields, which have no z components.

4 Discussion

The mean electromotive force in a turbulent fluid may have a part that is independent of the mean magnetic field and also independent of the mean flow. As an example we have studied forced hydromagnetic turbulence in a rotating body. In this case the Yoshizawa effect occurs, that is, a contribution $c_\Omega \boldsymbol{\Omega}$ to $\langle \mathbf{u} \times \mathbf{b} \rangle$. We have confirmed that c_Ω is determined by the mean cross-helicity $\langle \mathbf{u} \cdot \mathbf{b} \rangle$. We have also seen that, if an α effect is present, the Yoshizawa effect can to a large extent be compensated by the action of magnetic fields maintained by this α effect.

In astrophysics, the occurrence of non-zero cross-helicity is not a very common phenomenon. We give here a few examples in which the findings of this paper could be of interest. In the solar wind the systematic radial flow together with the Sun's large-scale magnetic field give rise to cross helicity of opposite sign in the two hemispheres. Although this primarily implies cross helicity associated with mean flow and mean magnetic field, it also results in cross helicity associated with the fluctuations. Together with the Sun's rotation, the latter should then produce a component of the mean electromotive force that is distinct

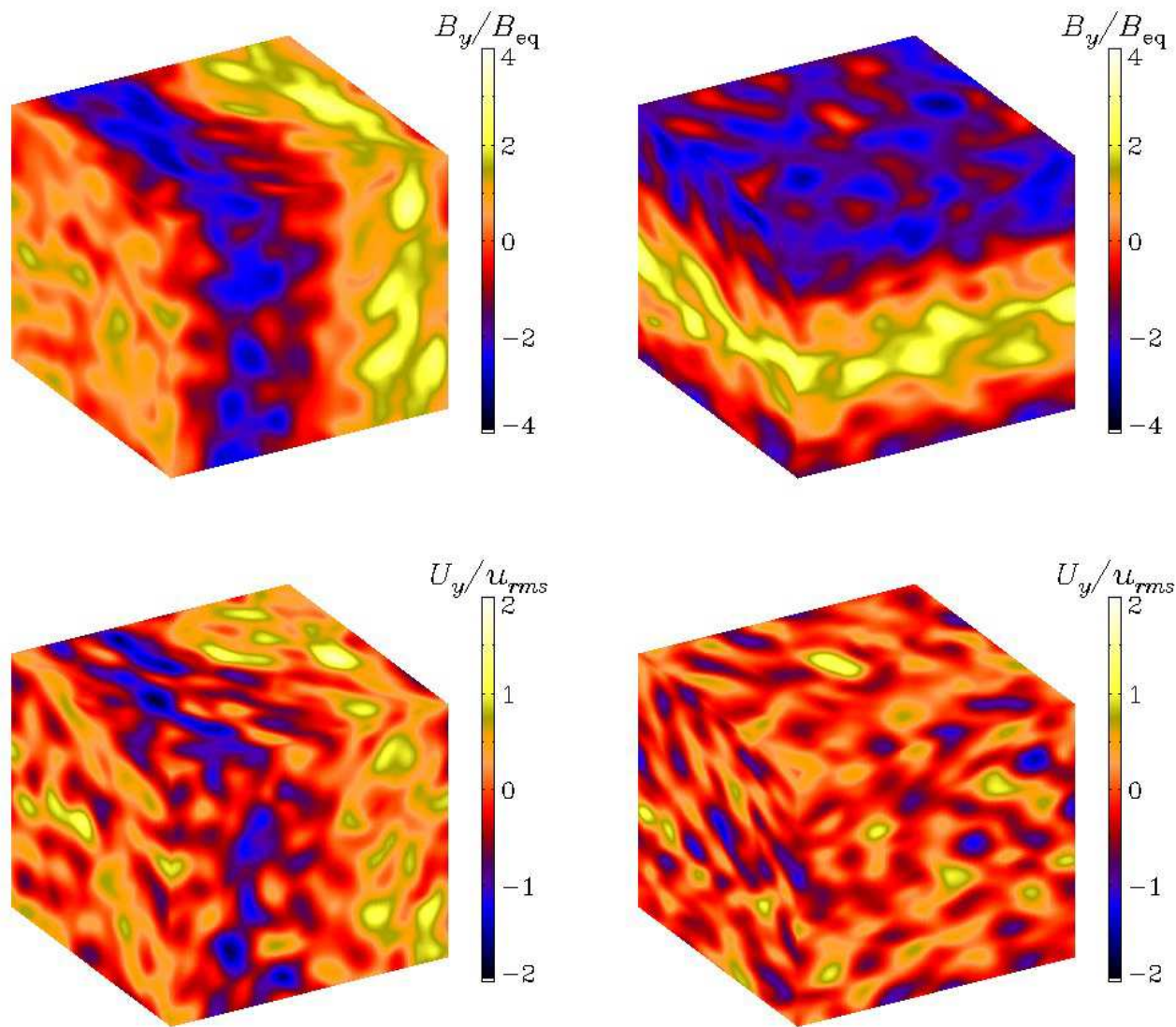


Figure 4. Helical case. Upper row: B_y/B_{eq} on the periphery of the computational domain, state with B^X type field (left) and B^Z type field (right), $\text{Co} = 0.37$. Lower row: same as above, but U_y/u_{rms} .

from that related to the α effect. Note, however, that the cross-helicity associated with the fluctuations is directly a consequence of the cross helicity from the large-scale field.

Another example where small-scale cross helicity can be generated is in a stratified layer with a vertical magnetic field (Rüdiger *et al.* 2011). Again, the sign of $\langle \mathbf{u} \cdot \mathbf{b} \rangle$ is linked to the orientation of the large-scale field relative to the direction of gravity.

Finally, cross helicity can be generated spontaneously and can then be of either sign, such as in the Archontis dynamo (Archontis 2000); for kinematic simulations see Archontis *et al.* (2003) as well as Cameron and Galloway (2006). Sur and Brandenburg (2009) have analyzed this dynamo with respect to the Yoshizawa effect. In this example too, large-scale and small-scale fields are intimately related. This interrelation means that whenever we expect the $\mathcal{E}^{(0)}$ term to be present in an astrophysical system, there should also be a mean magnetic field. Such an effect that is odd in the mean magnetic field might therefore instead just as well be associated with an α effect. As it turns out, this is also the case in the present simulations, where a large-scale magnetic field has been produced. In the present case, we have gone a step further by including also kinetic helicity also, in addition to just cross helicity. This produces an α effect and, as a consequence of this, a large-scale magnetic field. This field is particularly important when

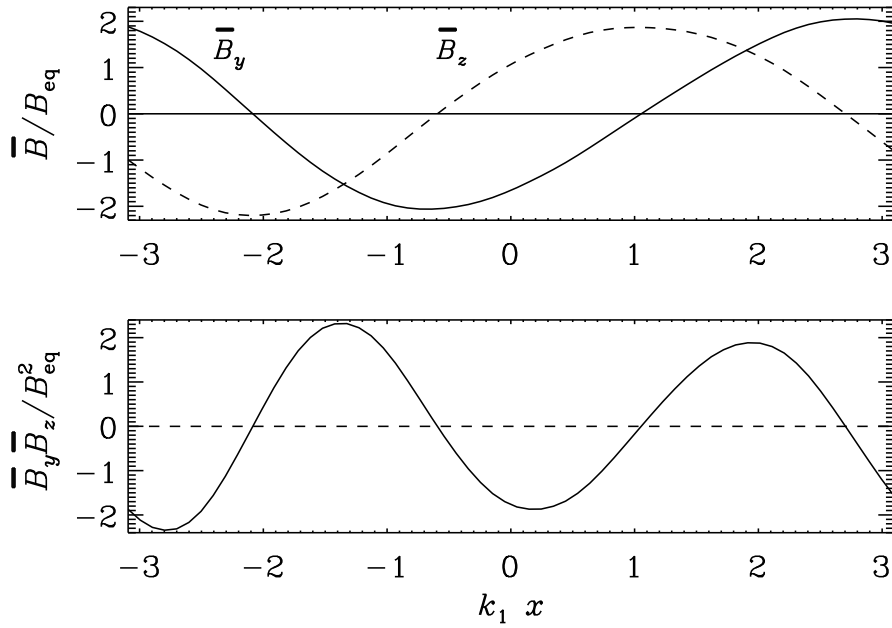


Figure 5. Helical case. Profiles of $\bar{B}_y(x)/B_{eq}$ and $\bar{B}_z(x)/B_{eq}$ as well as their product in a state with \mathbf{B}^Z field, $Co = 0.2$. Overbars denote yz averages. The dashed line gives the level of the x average of $\bar{B}_y \bar{B}_z / B_{eq}^2$, which is close to zero (here, $\approx -10^{-3}$).

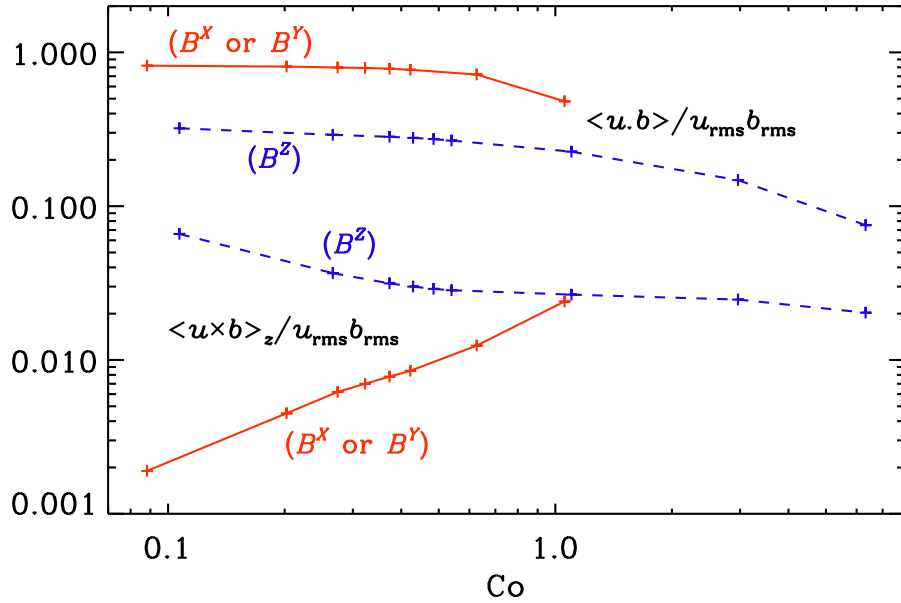


Figure 6. Helical case. Normalized cross helicity $\langle \mathbf{u} \cdot \mathbf{b} \rangle / u_{rms} b_{rms}$ (upper lines) and z component of the normalized mean electromotive force $\langle \mathbf{u} \times \mathbf{b} \rangle_z / u_{rms} b_{rms}$ (lower lines) as functions of Co ; the moduli of the x and y components are below 10^{-3} . Solid lines correspond to states with \mathbf{B}^X or \mathbf{B}^Y type fields, dashed lines to states with \mathbf{B}^Z type fields.

rotation is weak, because then the Yoshizawa effect is strongly quenched by this field.

Acknowledgements

We are grateful to Dr. Nobumitsu Yokoi for helpful comments on this paper. We acknowledge the allocation of computing resources provided by the Swedish National Allocations Committee at the Center for Parallel Computers at the Royal Institute of Technology in Stockholm and the National Supercomputer Centers in Linköping. This work was supported in part by the European Research Council under the AstroDyn

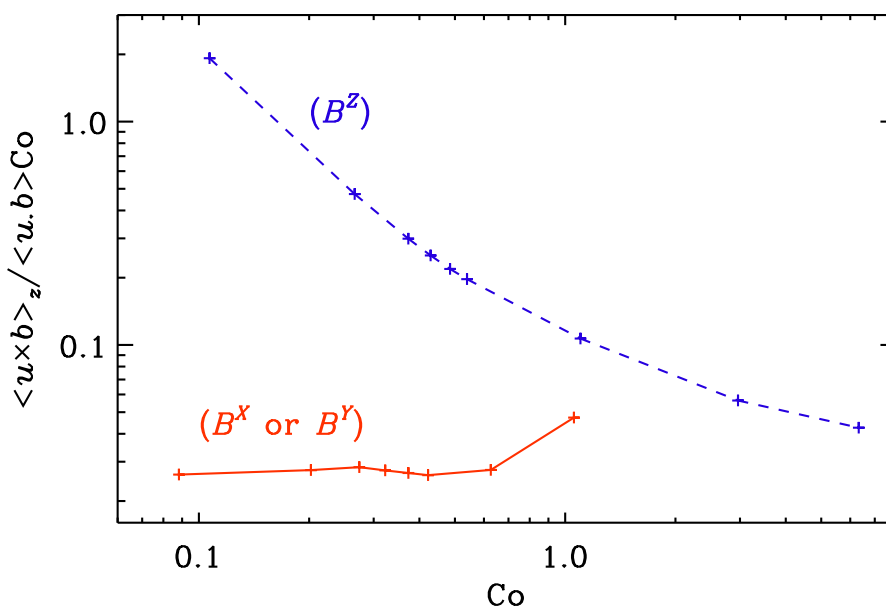


Figure 7. Helical case. Dependence of $\langle \mathbf{u} \times \mathbf{b} \rangle_z / \langle \mathbf{u} \cdot \mathbf{b} \rangle Co$ on Co . Solid lines correspond to states with B^X or B^Y type fields, dashed lines to states with B^Z type fields.

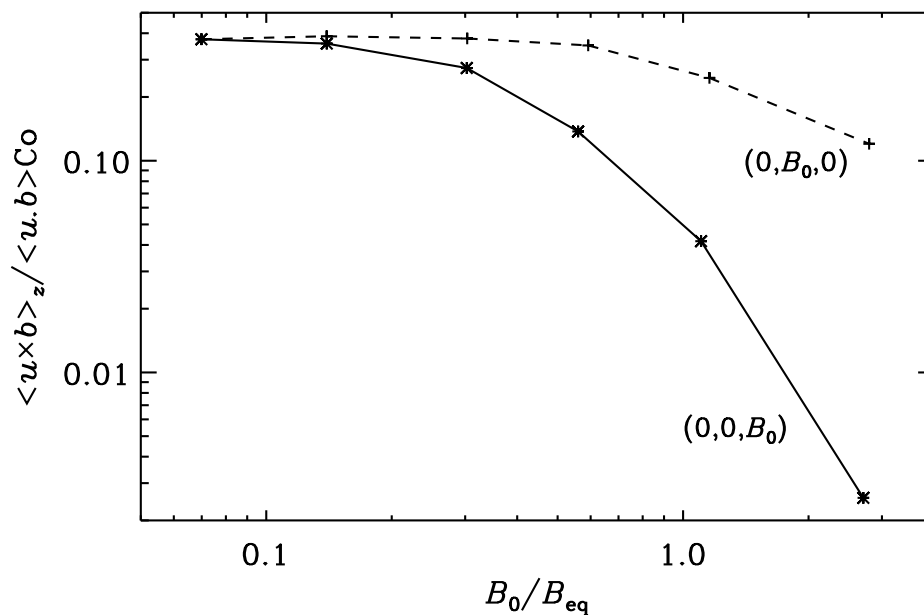


Figure 8. Non-helical case with an imposed homogeneous magnetic field in y or in z direction, $(0, B_0, 0)$ (dashed line) or $(0, 0, B_0)$ (solid line). Dependence of $\langle \mathbf{u} \times \mathbf{b} \rangle_z / \langle \mathbf{u} \cdot \mathbf{b} \rangle Co$ on B_0 / B_{eq} at $Co \approx 0.25$, $Re_M \approx 10$.

Research Project No. 227952.

REFERENCES

Archontis, V. *Linear, non-linear and turbulent dynamos*. Ph.D. Thesis, University of Copenhagen, Denmark (2000).
 Archontis, V., Dorci, S.B.F. and Nordlund, Å., “Numerical simulations of kinematic dynamo action,” *Astron. Astrophys.* **397**, 393-399 (2003).

- Brandenburg, A., "The inverse cascade and nonlinear alpha-effect in simulations of isotropic helical hydromagnetic turbulence," *Astrophys. J.* **550**, 824-840 (2001).
- Brandenburg, A. and Urpin, V., "Magnetic fields in young galaxies due to the cross-helicity effect," *Astron. Astrophys.* **332**, L41-L44 (1998).
- Cameron, R. and Galloway, D., "Saturation properties of the Archontis dynamo," *Monthly Notices Roy. Astron. Soc.* **365**, 735-746 (2006).
- Haugen, N.E.L., Brandenburg, A. and Dobler, W., "Simulations of nonhelical hydromagnetic turbulence," *Phys. Rev.* **70**, 016308 (2004).
- Hubbard, A., Del Sordo, F., Käpylä, P.J. and Brandenburg, A., "The α effect with imposed and dynamo-generated magnetic fields," *Monthly Notices Roy. Astron. Soc.* **398**, 1891-1899 (2009).
- Krause, F. and Rädler, K.-H. *Mean-field Magnetohydrodynamics and Dynamo Theory*. Oxford: Pergamon Press (1980).
- Moffatt, H.K. *Magnetic Field Generation in Electrically Conducting Fluids*. Cambridge: Cambridge Univ. Press (1978).
- Parker, E.N. *Cosmical magnetic fields*. Clarendon Press, Oxford (1979).
- Rädler, K.-H. and Brandenburg, A., "Mean electromotive force proportional to mean flow in mhd turbulence," *Astron. Nachr.* **331**, 14-21 (2010).
- Rheinhardt, M. and Brandenburg, A., "Test-field method for mean-field coefficients with MHD background," *Astron. Astrophys.* **520**, A28 (2010).
- Rüdiger, G., "On the α -effect for slow and fast rotation," *Astron. Nachr.* **299**, 217-222 (1978).
- Rüdiger, G., Kitchatinov, L. L. and Brandenburg, A., "Cross helicity and turbulent magnetic diffusivity in the solar convection zone," *Solar Phys.* **269**, 3-12 (2011).
- Sur, S. and Brandenburg, A., "The role of the Yoshizawa effect in the Archontis dynamo," *Monthly Notices Roy. Astron. Soc.* **399**, 273-280 (2009).
- Yokoi, N., "Large-scale magnetic-fields in spiral galaxies viewed from the cross-helicity dynamo," *Astron. Astrophys.* **311**, 731-745 (1996).
- Yokoi, N., "Modeling the turbulent cross-helicity evolution: production, dissipation, and transport rates," *J. Turb.* **12**, N27 (2011).
- Yoshizawa, A., "Self-consistent turbulent dynamo modeling of reversed field pinches and planetary magnetic fields," *Phys. Fluids B* **2**, 1589-1600 (1990).
- Yoshizawa, A. and Yokoi, N., "Turbulent magnetohydrodynamic dynamo effect for accretion disks using the cross-helicity effect," *Astrophys. J.* **407**, 540-548 (1993).
- Zeldovich, Ya. B., Ruzmaikin, A. A. and Sokoloff, D. D. *Magnetic fields in astrophysics*. Gordon & Breach, New York (1983).